Rutherford Scattering

Physics Lab 3+4 at ETH Zürich

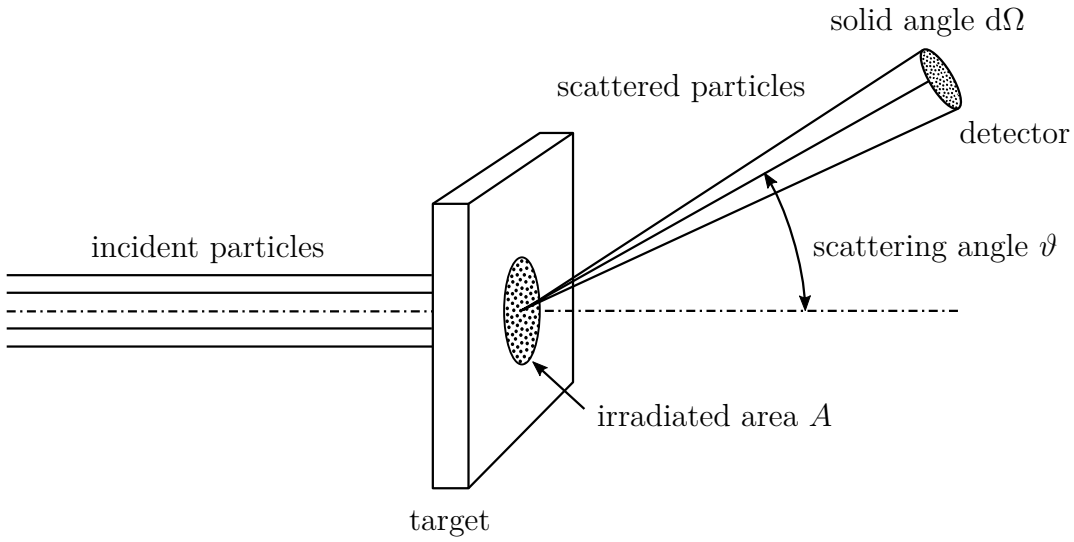

Author (Sep. 1999):	Reiner Mühle
Revision 1 (Jan. 2007):	Lukas Wacker
Revision 2 (Feb. 2021):	Niklas Bogensperger

Contents

1 Safety

⚠ The vacuum chamber may be only be opened by the assistant (radioactive ^{241}Am source!).
⚠ Observe general rules of conduct when handling radioactive substances!
⚠ Follow all other safety instructions at the setup or given by the assistants!

2 Introduction

In 1913, Geiger and Marsden [1] published the results of their research on the scattering of α particles by thin metal foils. These experiments brilliantly confirmed the hypothesis of the existence of a heavy positively charged nucleus within the atom put forward by Rutherford [2].

In these experiments, α particles (He^{2+} ions) of natural radioactive emitters were used as probes. These ions with energies in the MeV range can only be slightly deflected by interaction processes with the light electrons of the scattering atom. Large scattering angles, as observed experimentally, are only possible by scattering at the atomic nucleus.

Artificially accelerated ions were used to trigger nuclear processes from about 1932 onwards, after appropriate particle accelerators became available. The focus of this work was to explain the structure and level schemes of atomic nuclei and the nuclear transformations triggered by ion bombardment. Ion scattering was already used at that time to identify impurities in the bombarded target materials. However, the widespread use of ion scattering became possible only after semiconductor detectors became available for the detection of particle and quantum radiation. In conjunction with these detectors and through the use of small computers, low-energy accelerators became widely used analytical instruments. The use of ion scattering for analytical applications was greatly influenced by the introduction of ion implantation for the doping of semiconductors. This novel doping technology necessitated the measurement of defect and dopant depth profiles, which could be achieved using ion scattering [3]. Today, ion scattering, in particular the scattering of He ions with energies $E < 2\,\mathrm{MeV}$, is widely used to analyze near-surface regions of solids.

The main task of this experiment is to verify the angular dependence in Rutherford's scattering formula by determining the exponent of $\sin(\vartheta/2)$. Another goal is to acquire knowledge in the following areas:

- Kinematics of α decay: determination of the energy of α particles.
- Detector and measurement electronics (signal processing): detector (signal generation, energy resolution), discriminator (pulse shaper), counter.
- Interaction of charged particles with matter:
  - Elastic scattering as a single process: impact parameters, deflection angle, observation in both the laboratory and the center of mass system.
  - Elastic scattering as a collective process: cross section, differential cross section (transformation between the laboratory and center of mass system).
  - Specific energy loss: Bethe-Bloch formula, range, range dispersion, energy dispersion.
- Measurement acquisition and processing: optimal choice of measurement points and measurement times, statistical analysis, linear regression taking into account measurement errors, goodness-of-fit test (χ^2 test).

3 Theoretical Exercises

3.1 Kinetic energy of the α particles

- Calculate the kinetic energy $T_{\alpha i}$ of α particles emitted from a ^{241}Am source using the values for the excitation energies E_{Ai} given in table 1.
- From this, determine their mean energy T_m using the given transition probabilities.
- Calculate the mean kinetic energy $T_{m,c}$ of the α particles in the center of mass system (α particles - gold atom).
- From here on, the value $E_\alpha = 3.65\,\text{MeV}$ should be used for the energy of the α particles (see section 5.2.1). Why do the values from the tasks above differ from this one?

3.2 The closest possible approach D

- Calculate the closest possible approach D of the α particles to a gold nucleus using equation 26.
- Using equation 17, determine the differential cross section for this central impact.

3.3 Validity of the Rutherford formula

- Calculate the scattering angle ϑ (see figure 14) and the impact parameter b (see equation 2) for two different distances $x_{\min} = 50\,\text{mm}$ and $x_{\max} = 150\,\text{mm}$ between the scattering foil and the detector (assume that the particles are scattered at the height R_A).
- Examine whether deviations (for both high and low energies) from Rutherford's formula are to be expected when α particles are used in the energy range that is being considered (see chapter 7.1).

3.4 Specific energy loss

3.4.1 In the gold foil

- Using the Bethe-Bloch formula (see chapter 7.4), calculate the stopping power of α particles in gold in units of $\text{eV}/(10^{15}\text{atoms/cm}^2)$ and keV/µm. Use the constants given in table 4 for K and $\langle E_B \rangle$.
- Which energy of the α particles is available for signal formation in the semiconductor if the middle hole of the scattering geometry is used?
- For $x_{\min} = 50\,\text{mm}$, calculate the minimum and maximum energies $E_{\min}$ and $E_{\max}$ of the α particles in the scattering experiment which are available for signal formation in the detector, taking into account the finite dimensions of the scattering foil and detector (figure 14 may be useful).

3.4.2 In air

- Using the Bethe-Bloch formula (see chapter 7.4), calculate the stopping power of α particles in air in units of $\text{eV}/(10^{15}\text{atoms/cm}^2)$ and keV/mm. Does a chamber pressure of 5 to 10 mbar have an effect on the measurement or not?

3.5 Differential cross section $\sigma(\vartheta)$

- Calculate the correction factor that results for $\sigma(\vartheta)$ when we transform from the center of mass system to the laboratory system (i.e. the mass of the gold nucleus is not assumed to be infinite), see equations 13 and 15, and plot its behavior for all possible ϑ. Based on the results, what can be said about the further consideration of the correction factor?
- Calculate the differential cross section for Rutherford scattering for $x_{\min} = 50\,\mathrm{mm}$. What are the corrections compared to the assumption that all particles are scattered at the height of the central radius of the foil ring, when taking into account the finite dimensions of the scattering foil and detector (figure 14 might be useful)? Consider how a plot of these corrections to the nominal angle looks like and what this means for the experiment.

4 Fundamentals

4.1 Elastic scattering

We consider the elastic scattering of α particles at the unshielded Coulomb potential of Au nuclei (see figure 1). The α particle flies toward the target nucleus with velocity v_0 and impact parameter b and is deflected through the angle ϑ. The Au nucleus shall be at rest before the collision.

α particle	m_1	mass
	$Z_1 e$	charge ($Z_1 = 2$)
	v_0	velocity
	E_0	kinetic energy
Au nucleus	m_2	mass
	$Z_2 e$	charge ($Z_2 = 79$)

The potential in this situation is

$$V(r) = \frac{Z_1 Z_2 e^2}{4\pi\varepsilon_0}\frac{1}{r} = \frac{Z_1 Z_2 \xi^2}{r}\,, \tag{1}$$

where ξ^2 is a constant defined by $\xi^2 = \frac{e^2}{4\pi\varepsilon_0} = 1.44\,\mathrm{eV\,nm}$. In the repulsive Coulomb potential, the α particle describes a hyperbolic orbit [4]. For the scattering angle ϑ the following relation follows:

$$\tan\left(\frac{\vartheta}{2}\right) = \frac{Z_1 Z_2 \xi^2}{m_1 v_0^2 b} = \frac{Z_1 Z_2 \xi^2}{2E_0 b}\,. \tag{2}$$

Thus, for a given energy E_0, the impact parameter b uniquely determines the associated scattering angle ϑ.

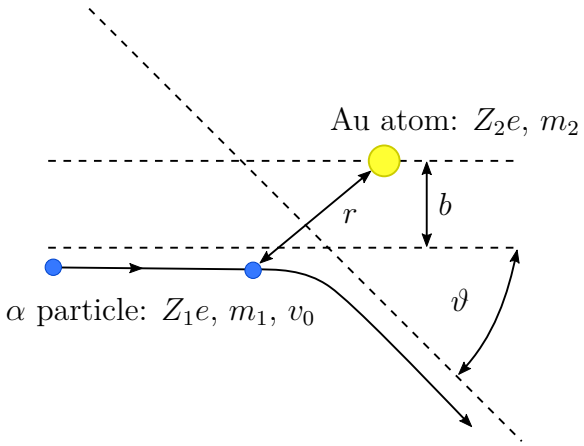

Figure 1: Elastic scattering.

The α particle transfers kinetic energy to the Au nucleus during the interaction. The kinetic energy E_1 of the α particle after the interaction can be calculated from the con-

servation laws of energy and momentum [3]. For the ratio E_1/E_0 we get:

$$\frac{E_1}{E_0} = K_2 = \left(\frac{K_1 \cos\vartheta + \sqrt{1 - K_1^2 \sin^2\vartheta}}{1 + K_1} \right)^2 , \tag{3}$$

where we defined $K_1 = \frac{m_1}{m_2}$ and call K_2 kinematic factor.

4.2 Cross section

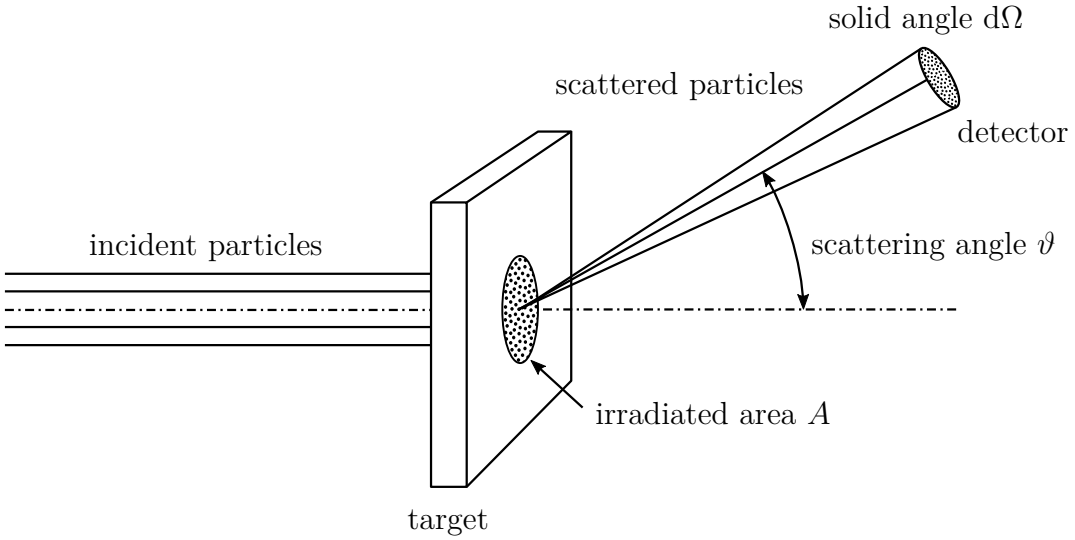

Figure 2: Scattering experiment.

To calculate the number of scattered particles as a function of the scattering angle, we need the concept of the cross section. A common scattering experiment is shown schematically in figure 2 [4]. A parallel beam of particles falls on a target and illuminates the area A. Under the angle ϑ against the direction of the incident beam there is a detector. It detects the particles leaving the target into the differential solid angle $\mathrm{d}\Omega$. We want to find the number of scattered particles registered by the detector per unit of time. Since no further direction shall be physically distinguished (e.g. by a spin or a magnetic field), the scattering intensity will not depend on the azimuth angle φ, but only on ϑ. The probability W (classical definition) that an elastic scattering occurs when irradiating the target surface A is given by

$$W = \frac{\mathrm{d}N_a/\mathrm{d}t}{\mathrm{d}N_e/\mathrm{d}t} = \frac{N_a/t}{N_e/t} = \frac{N_{\mathrm{AK}} \cdot \sigma}{A} = \frac{\text{number of scattering events per unit of time}}{\text{number of incident particles per unit of time}} . \tag{4}$$

Since the half-life of ^{241}Am is large compared to the duration of our experiment, we have stationary conditions in time. Therefore, we could replace the terms $\mathrm{d}N/\mathrm{d}t$ by N/t. Furthermore, we assigned a defined area σ to each scattering center (cross section). Whenever the center of mass of the incoming particle hits this area, scattering shall take place. The number of atomic nuclei (scattering centers) in the irradiated target volume $V = A \cdot d$ was denoted here by N_{AK}. We assumed here that the target thickness d is so small that the effective areas σ do not overlap. From equation 4, we thus obtain for σ:

$$\sigma = \frac{N_a/t}{N_{\mathrm{AK}} N_e/(At)} = \frac{\text{number of reactions per scattering center and unit of time}}{\text{current density of the incident particles}} . \tag{5}$$

For the probability $\mathrm{d}W(\vartheta)$, i.e. for the scattering into the differential solid angle $\mathrm{d}\Omega$ under the angle ϑ, we thus obtain:

$$\mathrm{d}W(\vartheta) = \frac{\mathrm{d}N_a/t}{N_e/t} = \frac{N_{\mathrm{AK}}\mathrm{d}\sigma(\vartheta)}{A} = \frac{N_{\mathrm{AK}}}{A}\frac{\mathrm{d}\sigma(\vartheta)}{\mathrm{d}\Omega}\mathrm{d}\Omega\,. \tag{6}$$

The quantity $\mathrm{d}\sigma/\mathrm{d}\Omega = \sigma(\vartheta)$ is called differential cross section. From equation 6 we get the following expression for it:

$$\frac{\mathrm{d}\sigma(\vartheta)}{\mathrm{d}\Omega} = \sigma(\vartheta) = \frac{\mathrm{d}N_a/\mathrm{d}\Omega}{N_{\mathrm{AK}}N_e/A} = \frac{\mathrm{d}N_a/(\mathrm{d}\Omega t)}{N_{\mathrm{AK}}j}\,, \tag{7}$$

which means:

$$\frac{\mathrm{d}\sigma(\vartheta)}{\mathrm{d}\Omega} = \frac{\text{number of particles scattered in } \mathrm{d}\Omega \text{ per unit of time}}{\text{number of target nuclei} * \text{current density of incident particles}}\,. \tag{8}$$

The quantity $j = N_e/(At)$ is the current density of the incident particles. Equations 5 and 7 can be regarded as definitions of the cross sections. They are also useful for quantum mechanical problems. By integrating $\sigma(\vartheta)$ over the total solid angle, we obtain the total cross section σ_{tot}. In nuclear physics, cross sections for nuclear reactions are defined analogously. The cross section has the dimension of an area. The common unit is barn,

$$1\,\mathrm{barn} = 10^{-24}\,\mathrm{cm}^2\,, \tag{9}$$

since the values of many cross sections lie within this order of magnitude. The unit for the differential cross section is accordingly e.g. barn/sr or mbarn/sr.

4.3 Cross section for elastic scattering

To calculate the cross section for elastic scattering, we first consider equation 2. The scattering angle ϑ is a unique function of the impact parameter b and the particle energy E, i.e.: $\vartheta = \vartheta(b, E)$. All particles which asymptotically emerge from an annulus between b and $b+\mathrm{d}b$ around the symmetry axis are scattered into the solid angle $\mathrm{d}\Omega = 2\pi\sin(\vartheta)\mathrm{d}\vartheta$ and must find themselves there, i.e.:

$$j \cdot 2\pi b\mathrm{d}b = j \cdot \mathrm{d}\Omega\frac{\mathrm{d}\sigma}{\mathrm{d}\Omega} = j \cdot 2\pi\sin(\vartheta)\mathrm{d}\vartheta\frac{\mathrm{d}\sigma(\vartheta)}{\mathrm{d}\Omega}\,, \tag{10}$$

or

$$\frac{\mathrm{d}\sigma(\vartheta)}{\mathrm{d}\Omega} = \frac{b}{\sin\vartheta}\left|\frac{\mathrm{d}b}{\mathrm{d}\vartheta}\right|. \tag{11}$$

In equation 11 we have an absolute value because by definition the cross section cannot become negative. We can solve equation 2 for b and get:

$$b = \frac{Z_1 Z_2 \xi^2}{2E}\frac{1}{\tan\left(\frac{\vartheta}{2}\right)}\,, \tag{12}$$

and with equation 11 after some rearranging:

$$\boxed{\sigma(\vartheta) = \frac{\mathrm{d}\sigma(\vartheta)}{\mathrm{d}\Omega} = \left(\frac{Z_1 Z_2 \xi^2}{4E}\right)^2 \frac{1}{\sin^4\left(\frac{\vartheta}{2}\right)}}\,. \tag{13}$$

This is Rutherford's famous scattering formula.

If the scattering center does not have infinite mass, equation 13 is valid in center of mass coordinates. The energy and the scattering angle are then the quantities in the center of mass system (highlighted by the index c):

$$E_{1c} = \frac{m_1}{2} v_{1c}^2 = \left(\frac{m_2}{m_1 + m_2}\right) \frac{1}{2} m_r v_r^2 = \frac{E_0}{(1 + K_1)^2}\,, \tag{14}$$

with v_r the relative velocity between the two particles, which in our case coincides with the particle velocity v_0 in the laboratory system, since the gold nucleus is at rest before the collision, $m_r = \frac{m_1 m_2}{m_1 + m_2}$ the reduced mass, and $\tan\vartheta = \frac{\sin\vartheta_c}{K_1 + \cos\vartheta_c}$ the relation between the scattering angles. The transformation of equation 13 into the laboratory system results in [3]

$$\sigma(\vartheta) = \frac{\mathrm{d}\sigma(\vartheta)}{\mathrm{d}\Omega} = \left(\frac{Z_1 Z_2 \xi^2}{4E}\right)^2 \frac{4}{\sin^4\vartheta} \frac{\left(\cos\vartheta + \sqrt{1 - \left(\frac{m_1}{m_2}\sin\vartheta\right)^2}\right)^2}{\sqrt{1 - \left(\frac{m_1}{m_2}\sin\vartheta\right)^2}}\,. \tag{15}$$

For $m_1 \ll m_2$, $\sigma(\vartheta)$ can be expanded into a power series:

$$\sigma(\vartheta) = \left(\frac{Z_1 Z_2 \xi^2}{4E}\right)^2 \left(\sin^{-4}\left(\frac{\vartheta}{2}\right) - 2\left(\frac{m_1}{m_2}\right)^2 + \ldots\right), \tag{16}$$

where the first omitted term is of order $\left(\frac{m_1}{m_2}\right)^4$. If we express the energy in terms of MeV, $\sigma(\vartheta)$ has the following expression:

$$\sigma(\vartheta) = 1.296\left(\frac{Z_1 Z_2}{E/\mathrm{MeV}}\right)^2 \left(\sin^{-4}\left(\frac{\vartheta}{2}\right) - 2\left(\frac{m_1}{m_2}\right)^2 + \ldots\right)\mathrm{mbarn/sr}\,. \tag{17}$$

The total cross section for elastic scattering equals ∞, since we have assumed an infinite range for the Coulomb force.

4.4 Relationship with the measured variables

From equation 6 we obtain for the particles emitted in $\mathrm{d}\Omega$:

$$\mathrm{d}N_a = \frac{N_{\mathrm{AK}} t}{A} \frac{N_e}{t} \frac{\mathrm{d}\sigma}{\mathrm{d}\Omega} \mathrm{d}\Omega\,. \tag{18}$$

However, since our detector has a finite size, we still have to integrate over its solid angle Ω_D:

$$N_a = \frac{N_{\mathrm{AK}} t}{A} \frac{N_e}{t} \int_{\Omega_D} \frac{\mathrm{d}\sigma}{\mathrm{d}\Omega} \mathrm{d}\Omega = n_{\mathrm{AK}} t d \frac{N_e}{t} \Omega_D \frac{\mathrm{d}\sigma}{\mathrm{d}\Omega} = n_{\mathrm{AK}} t d I_S \frac{\Omega_F}{4\pi} \Omega_D \left(\frac{Z_1 Z_2 \xi^2}{4E}\right)^2 \frac{1}{\sin^4\left(\frac{\vartheta}{2}\right)} \tag{19}$$

Here Ω_F is the solid angle under which the source sees the scattering foil, see equation 41. And thus

$$\frac{N_a}{\Omega_D t} = \frac{C}{\sin^4\left(\frac{\vartheta}{2}\right)}\,, \tag{20}$$

or respectively

$$\boxed{\ln\left(\frac{N_a}{\Omega_D t}\right) = \ln C - 4\ln\left(\sin\left(\frac{\vartheta}{2}\right)\right)}\,. \tag{21}$$

The constant

$$C = n_{\mathrm{AK}} d I_S \frac{\Omega_F}{4\pi}\left(\frac{Z_1 Z_2 \xi^2}{4E}\right)^2 \tag{22}$$

can be determined experimentally. I_S is the activity of the Am source, d the thickness of the foil, and n_{AK} the bulk density of the gold atoms. Equation 21 has the form of a straight line equation $y = ax + b$, where

$$y = \ln\left(\frac{N_a}{\Omega_D t}\right), \quad x = \ln\left(\sin\left(\frac{\vartheta}{2}\right)\right), \quad a = -4\,. \tag{23}$$

If the measurements lie on this straight line, it would be the confirmation of the assumption that there are atomic nuclei in the center of the atoms, where the scattering takes place. The constant C can be determined from the intersection of the straight line with the ordinate. From the value of C the activity I_S of the Am source can be estimated, since the other quantities are known.

5 Measurement Apparatus

5.1 Structure of the apparatus

The apparatus we use is shown schematically in figure 3. In an evacuable glass cylinder (scattering chamber) the following are arranged on the same axis: α source, annular scattering foil and α detector. The chamber can be purged with a diaphragm pump down to a pressure of about 5 mbar, to avoid unwanted energy losses and scattering of α particles by gas molecules. The source and scattering foil are mounted at a fixed distance δ on a rotatable and movable metal rod. By rotating it, the source and/or a central hole in the foil plane can be uncovered. This makes it possible to measure the background while the source is covered. With the source and central hole of about 1 mm diameter open (covered with the same gold foil as the scattering foil), α particles can be shot directly at the detector. For the scattering measurements, the center hole can be closed. Further processing of the detector pulses is done with the electronic components outside the scattering chamber.

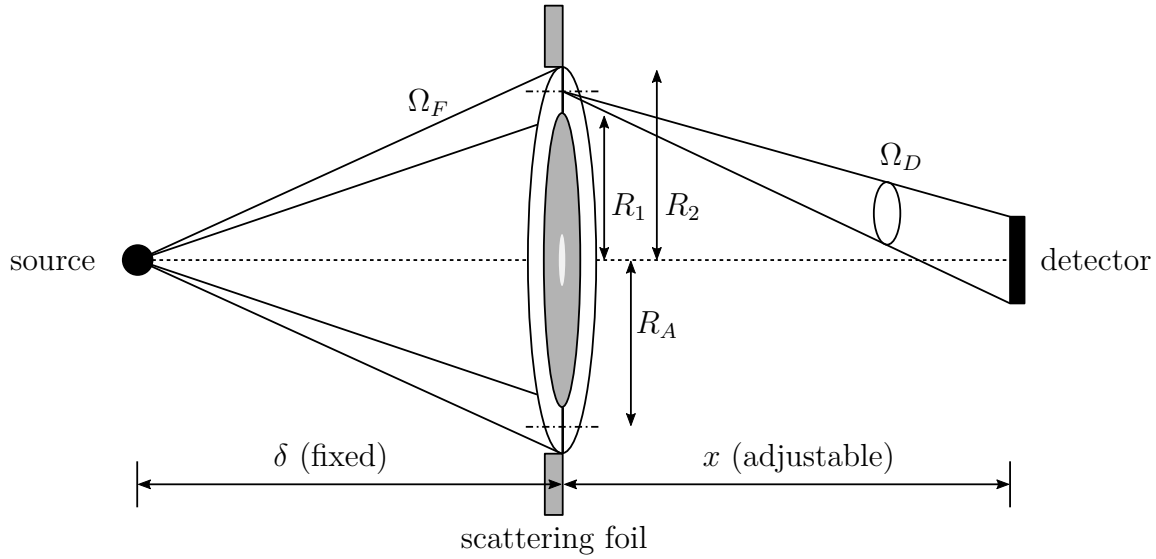

Figure 3: Scattering geometry. The fixed quantities are given as follows: $\delta = 73\,\text{mm}$, $R_1 = 23\,\text{mm}$, $R_2 = 27\,\text{mm}$, $R_A = 25\,\text{mm}$. Note: δ is measured from the source to the scattering foil, which is placed on the rear side of the indicated metal carrier disk (gray rectangles at the top and bottom). Furthermore, the small coverable hole in the center of the carrier disk is indicated.

5.2 Specifications of the components

5.2.1 Source

A ^{241}Am specimen is used as the α source. A thin layer of americium (mixed with silver) was deposited on a metal foil, onto which about 3 µm gold was then vapor-deposited. The half-life of ^{241}Am is 432 y and consequently we consider the source to have a constant activity I_S. During decay, α particles of different energies are emitted, which can be counted with the available detection equipment, but cannot be separated energetically. The α particles from the source we use, unlike a thin source such as those used in the VP on alpha absorption (see figure 9), show a broad energy distribution, with an average energy

of about 3.65 MeV and a full width at half maximum (FWHM) of about 840 keV, see figure 4. The reduced average energy increases the count rate of the scattering measurements (explanation!). The source is fixed on a metal plate and thus can emit into a solid angle of 4π. The diameter of the source is about 10 mm, but the activity is not uniformly distributed over the active area. We therefore assume the source to be point-like. The consequence for the calculation of the scattering angles can be easily estimated. The radioactive material used has the inconvenient property that larger conglomerates can enter the chamber through corrosion and recoil effects. This can lead to contamination of the scattering chamber and increase the background. It is therefore necessary to close the lid in front of the source after measurements and during longer measurement pauses.

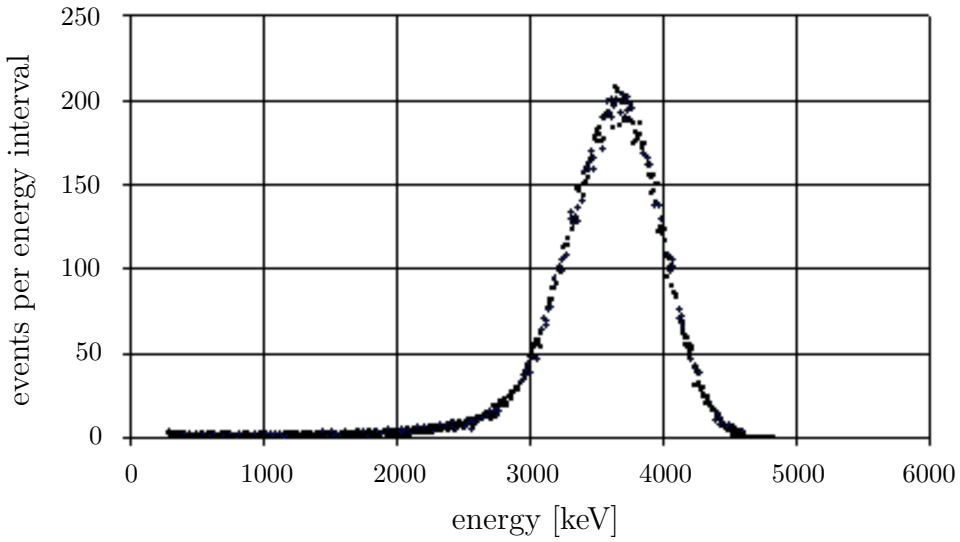

Figure 4: Energy distribution of the α particles of the ^{241}Am source we use. The average energy is 3.65 MeV, the full width at half maximum is 840 keV.

5.2.2 Scattering foil

In the experiment, a ring-shaped scattering foil made of gold is used. The ring geometry offers the advantage that with a good definition of the scattering angle a relatively large effective target area is involved in the scattering experiment (relatively large solid angle Ω_F). The use of gold as scattering foil is advantageous because the yield N_a of scattered particles increases with Z_2^2. The gold foil was produced by vapor deposition in vacuum. From the surface thickness ρ_F indicated on the glass cylinder used in the experiment setup, the geometric thickness $d = \rho_F/\rho$ equals about 1 µm (ρ is the material density). Therefore, great care must be taken when evacuating or venting the scattering chamber.

5.2.3 Detector

A surface barrier detector is used to detect α particles. It consists of a silicon single crystal (n-type) on whose surface a thin gold layer has been vapor-deposited. The key parameters can be found in the data sheet in figure 5.

QUALITY ASSURANCE DATA
Semiconductor Radiation Detectors

WARRANTY BASIS		ACTUAL MEASUREMENTS	
Shipment Date 7-15-81 Serial No. 21-267-F		Alpha Resolution 12.6	KeV FWHM[a]
Model No. CA-23-50-100		Noise width 5.4	KeV FWHM[b]
Active Area (nominal) 50	mm²	Shaping Time Constant 0.5	μs
5.486 MeV Alpha Resolution 23	KeV FWHM[a]	Reverse Current .12 μamps @ 85	volts
Noise width 17	KeV FWHM[b]	Temperature 21	°C
Temperature 22°C		Sensitive Thickness ≥100	microns
Shaping Time Constant 0.5	μs	Nominal Resistivity 4.4K	Ωcm
Sensitive Depth (minimum) ≥100	microns	Electrode Thickness: Au 40.0	μgm/cm²
Operating Bias 85	volts	Al 39.0	μgm/cm²
Pos ☑ Neg ☐			

Figure 5: Data sheet of the surface barrier detector.

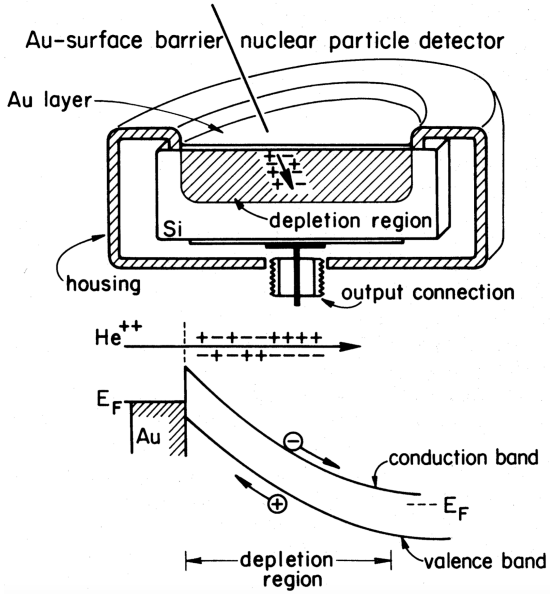

Figure 6: Schematic diagram of a surface barrier detector. The upper portion of the figure shows a cutaway sketch of the silicon disc with gold film mounted in the detector housing. The lower portion shows an α particle forming holes and electrons over its penetration path. The energy band diagram of a reverse-biased detector (positive polarity on n-type silicon) shows the electrons and holes being swept apart by the high electric field within the depletion region. (From [3].)

The resistivity of the silicon used is 4400 Ω cm. At the applied bias voltage of about 12 V, the sensitive layer has a thickness of about 120 µm [5], which is sufficient to decelerate α particles with energy greater than 10 MeV. In addition to the existing gold layer of 40 µg/cm^2, the detector was vapor-coated with a gold layer of about 200 µg/cm^2 to make it insensitive to light. This causes the α particles, similar to what happens in the scattering foil, to lose more or less energy depending on the scattering angle, which can lead to counting losses, especially at high discriminator settings. Furthermore, the energy resolution of the detector is worsened such that the individual α particle groups can no longer be separated, but this is not necessary in this experiment. When calculating the x value, note that the sensitive area of the detector ($A_D = 50\,\text{mm}^2$) is 3 mm behind the leading

edge of the detector. So 3 mm must be added to the measured distance (scattering foil - detector leading edge).

5.2.4 Electronics

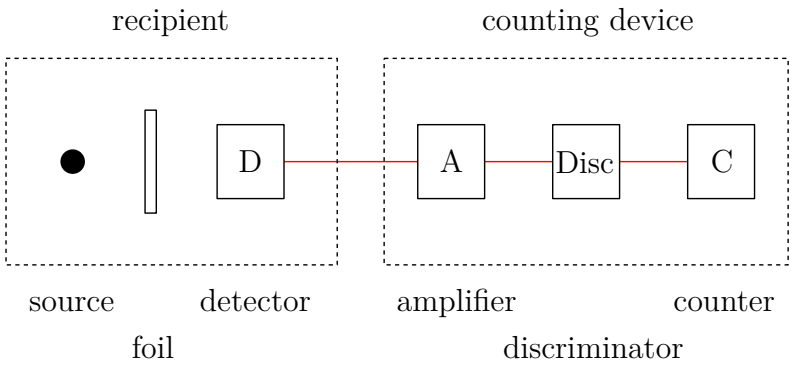

Figure 7: Block diagram of the electronic measuring equipment.

The block diagram of the electronic measuring equipment is shown in figure 7. The α particles hitting the detector D generate a charge pulse whose amplitude Q_I is proportional to the energy E_α deposited in the sensitive layer of the detector. A voltage pulse is generated, whose amplitude U_I is proportional to Q_I and consequently to the energy E_α. With the helical potentiometer on the discriminator we can set a level U_D which causes only those pulses to be allowed to pass whose amplitude U_I is greater than this level. Thus all background pulses can be filtered out. Furthermore, square pulses of constant amplitude U_Z are formed for the counter, whose width T_Z corresponds to the pulse width at the discriminator level. Therefore, even a too low discriminator level can cause that no more pulses are counted. This can then be seen in the discriminator curve.

6 Experimental Exercises and Procedure

6.1 Evacuation of the scattering chamber

At the beginning of the experiment, the scattering chamber must always be evacuated. Note that the scattering foil is very thin (µm range) and therefore very sensitive to strong gas flows. During the experiment, also monitor the pressure in the scattering chamber. If necessary, evactuate the chamber again. Switch off the pump when it is no longer needed.

Be sure to follow all guidelines posted at the workstation and the instructions given by the assistants!

6.2 Discriminator curve

Record the integral pulse height spectrum (discriminator curve) using the direct α beam. Proceed as follows:

- Open the lid of the source and the center hole by rotating the rod. Move the rod to the position nearest to the detector.
- Look at the waveform after the amplifier with the oscilloscope.
- Measure the count rate $z = N/t$ (N = number of pulses, t = measurement time) as a function of the discriminator setting U_D (measured in turns of the adjusting screw (arbitrary unit) or in volts, depending on the discriminator device).
- Plot z as a function of U_D (discriminator curve) and determine from it the pulse height spectrum ($\mathrm{d}z/\mathrm{d}U_D$ as a function of U_D) and the energy distribution of the α particles (number versus energy). The function

$$f(z; A, B, C) = A \operatorname{erfc}\left(\frac{z - B}{C\sqrt{2}}\right) \tag{24}$$

  with the complementary error function erfc and its parameters B = mean and C = standard deviation (identical to the parameters of a normal distribution associated with it) might be helpful.
- Compare the resulting energy distribution curve with the given one (see section 5.2.1) by equating the two mean values and comparing the standard deviations (convert the given FWHM). For this purpose the zero point must be chosen in such a way that the noise level of the discriminator is just below it.
- Choose the operating point (discriminator setting U_{DA}) for the following scattering measurements such that only the "correct" α particles are counted. Note that the location of the peak may still change with the scattering angle (why?).

6.3 Background radiation

Measure the background radiation of the setup and the surrounding area. Proceed as follows:

- Close the lid of the source and the center hole by rotating the rod. Move the rod to the position furthest away from the detector.
- Measure the count rate $z = N/t$ for approx. 1 hour.
- Decide whether this value must be taken into account in the other measurements.

6.4 Angular distribution

Verify the result of Rutherford's scattering formula. Proceed as follows:

- Open the lid of the source and close the lid of the center hole by rotating the rod.
- Measure the scattering rate for at least twelve (and at most 22) x values in the range between $x_{\min} = 50\,\text{mm}$ and $x_{\max} = 150\,\text{mm}$. Select the position of the measurement points such that they are equidistant to each other in the final plot (logarithm). For example, the outer points in the measurement area contribute much more to the accuracy than points near the center.
- Plot the angular distribution $N_a/(\Omega_D \cdot t) = f(\vartheta)$. Discuss the result.
- Record the measured values with the corresponding measurement errors in a double logarithmic plot. Determine the parameters a and b and their errors σ_a and σ_b by calculating the regression curve $y = ax + b$. The parameter a is the value of the exponent of $\sin(\vartheta/2)$ in Rutherford's scattering formula, which in theory should equal -4. Consider that in this case both x and y are subject to errors.
- Check the quality of your measurement results and linear fit with the χ^2 test [6] and determine the confidence interval of the parameters over χ^2.

6.5 Activity of the source

Find the activity in becquerel (Bq) and curie (Ci) of the ^{241}Am source in two different ways and compare the results:

- Take the measurement result (at the operating point) from the above section on the discriminator curve and extrapolate it to the whole space (when measuring only a limited solid angle is considered).
- Determine the activity I_S from the results of the previous section using equation 22.

7 Additional Topics

7.1 Deviations from Rutherford's scattering formula

Deviations from the scattering formula can occur at both low and high α energies. The derivation of Rutherford's scattering formula is based on the assumption that there is a Coulomb interaction of two unshielded point charges $Z_1 e$ and $Z_2 e$. Thus, it is assumed that the particle velocity is sufficiently large to allow the particle to penetrate deeply into the electron shell of the atoms and hence that the shielding of the nuclear charge by the electron shell does not matter. The total energy of the relative motion is $E_r = \frac{E_0}{1+K_1}$. Very small impact parameters can be obtained at high energies. Deviations from the scattering formula occur when the closest possible approach D, achievable with a central collision ($\vartheta = 180°$), comes within the range of nuclear forces. At the inversion point, the potential and kinetic energies are equal:

$$\frac{Z_1 Z_2 \xi^2}{D} = E_r = \frac{E_0}{1+K_1}\,, \tag{25}$$

thus

$$D = \frac{Z_1 Z_2 \xi^2 (1+K_1)}{E_0}\,. \tag{26}$$

Since the nuclear forces have an extremely short range, deviations from Rutherford's scattering formula occur when D reaches the order of magnitude of the nuclear radii. The nuclear radius R_K is directly proportional to the nucleon number $A = N + Z$ in the nucleus, with Z = proton number and N = neutron number. Assuming a spherical nucleus, this equals [4]:

$$R_K = r_0 A^{1/3}\,. \tag{27}$$

As early as 1935, the Rutherford scattering experiments yielded [4] for r_0 the value of

$$r_0 = (1.3 \pm 0.1) \times 10^{-13}\,\mathrm{cm} = (1.3 \pm 0.1)\,\mathrm{fm}\,. \tag{28}$$

Thus, we expect deviations to occur beyond particle energies for which $D = R_{K1} + R_{K2}$, i.e.:

$$E_r = \frac{Z_1 Z_2 \xi^2}{r_0\left(A_1^{1/3} + A_2^{1/3}\right)}\,. \tag{29}$$

At low energies, the particles cannot get sufficiently close to the nucleus, and its charge is partially shielded by electrons. The energies at which such shielding effects occur can be easily estimated. We require that the closest possible approach D must be smaller than the orbital radius $a_1 = \frac{a_0}{Z_2}$ of the electrons in the K shell. Here $a_0 = 52.9\,\mathrm{pm}$ is the Bohr radius. Thus we obtain the condition

$$E_r > \frac{Z_1 Z_2^2 \xi^2}{a_0}\,. \tag{30}$$

However, it turns out that already at larger energies than estimated by equation 30, deviations from the Rutherford cross section occur, since there are always some particle trajectories that lie in a region where the nuclear charge is shielded by the electrons. However, equation 30 can serve as a rough estimate.

7.2 Energy balance of the α decay

A layer of ^{241}Am (americium) is used as the source of α particles in the experiment. ^{241}Am is unstable via α decay with a half-life of 432 y.

$$^{241}\mathrm{Am} \implies {}^{237}\mathrm{Np}^{*} + \alpha\,. \tag{31}$$

The residual nucleus is ^{237}Np (neptunium), which in turn may remain in an excited state with discrete excitation energy E_A. This energy is usually emitted in the form of electromagnetic radiation. The kinetic energy T of the emitted particles can be calculated by taking into account energy and momentum conservation. We initially assume an infinitely thin source.

7.2.1 Energy balance

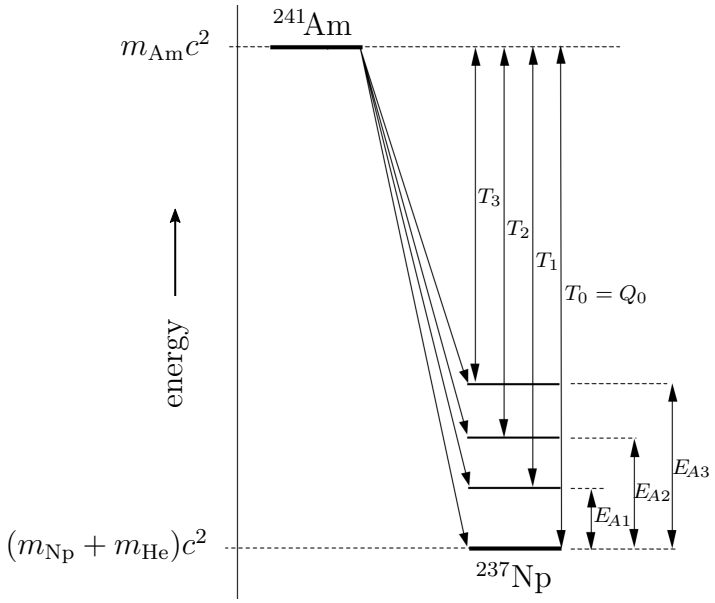

Figure 8: Energy balance of the α decay of ^{241}Am.

The diagram showing the energy balance of the α decay can be seen in figure 8. In radioactive decay, the total energy is conserved. Therefore, we can establish the following balance equation:

$$\mathrm{m}(^{241}\mathrm{Am})c^2 = \Big(\mathrm{m}^{*}(^{237}\mathrm{Np}) + \mathrm{m}(^{4}\mathrm{He})\Big)c^2 + T = \Big(\mathrm{m}(^{237}\mathrm{Np}) + \mathrm{m}(^{4}\mathrm{He})\Big)c^2 + E_A + T\,, \tag{32}$$

$$Q_0 = \Big(\mathrm{m}(^{241}\mathrm{Am}) - \mathrm{m}(^{237}\mathrm{Np}) - \mathrm{m}(^{4}\mathrm{He})\Big)c^2\,. \tag{33}$$

Here $\mathrm{m}^{*}(X)c^2 = \mathrm{m}(X)c^2 + E_A$ is the rest energy of the excited nucleus X. Q_0 is called decay energy. It is the maximum value of kinetic energy T available. The masses of the neutral atoms are to be used here. For simplicity, we write: $\mathrm{m}(^{241}\mathrm{Am}) = \mathrm{m}_{\mathrm{Am}}$, etc. So we have

$$T = Q_0 - E_A = T_\alpha + T_{\mathrm{Np}}\,. \tag{34}$$

Due to the discrete values E_{Ai} of the excitation energy of the residual nucleus, different groups of α particles with discrete energies $T_{\alpha i}$ are also emitted:

$$T_i = Q_i = Q_0 - E_{Ai} = T_{\alpha i} + T_{\mathrm{Np}i}\,. \tag{35}$$

The kinetic energy T_i is distributed between the α particle and the residual nucleus.

7.2.2 Momentum balance

Since the decay occurs from a stationary ^{241}Am nucleus, we obtain:

$$0 = \vec{p}_\alpha + \vec{p}_{\mathrm{Np}}\,, \tag{36}$$

thus

$$p_\alpha^2 = p_{\mathrm{Np}}^2\,, \quad T_{\mathrm{Np}} = \frac{m_\alpha T_\alpha}{m_{\mathrm{Np}}}\,. \tag{37}$$

And so we have:

$$T_{\alpha i} = \frac{Q_i}{1 + \frac{m_\alpha}{m_{\mathrm{Np}}}} = \frac{Q_0 - E_{Ai}}{1 + \frac{m_\alpha}{m_{\mathrm{Np}}}}\,. \tag{38}$$

The intensities $I_{\alpha i}$ of the most intense α groups are given in table 1.

Table 1: Excitation energies and transition probabilities for the α decay of ^{241}Am into ^{237}Np.

i	**0**	**1**	**2**	**3**	**4**
E_{Ai} [keV]	0	33.20	59.54	102.96	158.51
$I_{\alpha i}$ [%]	0.34	0.22	84.5	13.0	1.6
$T_{\alpha i}$ [MeV]					

The blank line should be completed by the reader, see theoretical exercises in chapter 3.1. The required values for the masses are given in table 2 in atomic mass units u ($1\,\mathrm{u\,c^2} = 931.49432\,\mathrm{MeV}$).

Table 2: Masses of the particles involved in α decay.

Atom / Particle	**Mass** [u]
α	4.001487900
^{4}He	4.002603250
^{237}Np	237.048167253
^{241}Am	241.056822944

Figure 9 shows the energy distribution of α particles as measured in the VP Alpha I experiment. Here, a "thin" α source is used (specific data not provided). The peaks have a width of about 20 keV, which is mainly due to the detector and electronics. The distribution shows the main group with a share of about 85 percent and the three other groups, which are particularly clearly visible in the logarithmic plot.

7.3 Solid angle

The solid angle $\mathrm{d}\Omega$ under which an area element $\mathrm{d}A$ is seen from a reference point 0 at distance r is calculated to be (see figure 10):

$$\mathrm{d}\Omega = \frac{\mathrm{d}\vec{A} \cdot \vec{e_r}}{r^2}\,. \tag{39}$$

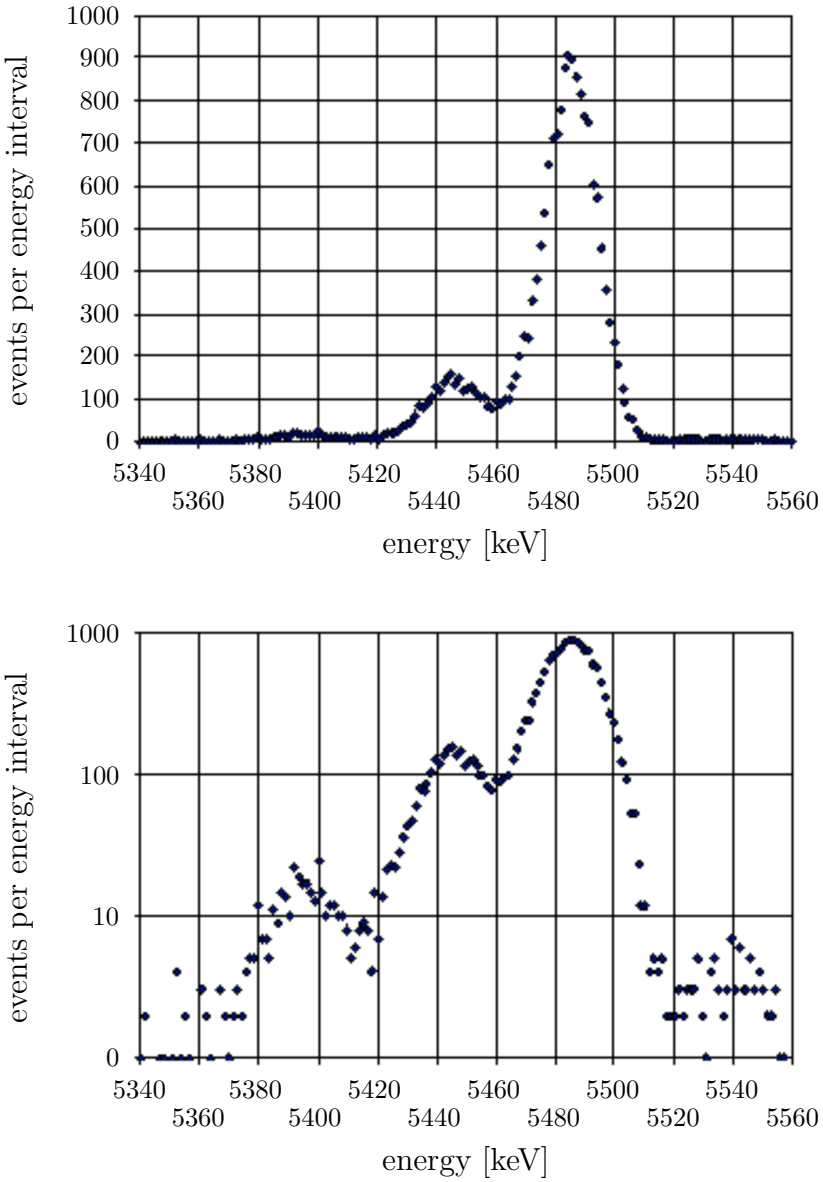

Figure 9: Energy distribution of α particles originating from a thin Am source. Top: Ordinate linear. Bottom: Ordinate logarithmic.

The total solid angle Ω is obtained by integration over the total area A:

$$\Omega = \int_A \mathrm{d}\Omega \quad \text{where} \quad [\Omega] = \mathrm{sr}\,. \tag{40}$$

To calculate the number of α particles hitting the detector, we additionally need the solid angles Ω_F and Ω_D (see figure 3).

7.3.1 Calculation of Ω_F

The solid angle under which the source sees the scattering foil can be easily calculated due to the cylinder symmetry at hand. With $\mathrm{d}A = 2\pi r \mathrm{d}r$ we obtain:

$$\Omega_F = 2\pi\left(\left(1+(R_1/\delta)^2\right)^{-1/2} - \left(1+(R_2/\delta)^2\right)^{-1/2}\right) = 0.0998\,\mathrm{sr}\,. \tag{41}$$

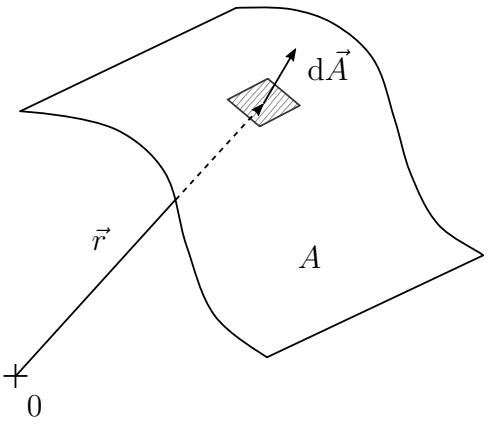

Figure 10: Definition of the solid angle.

7.3.2 Calculation of Ω_D

The calculation of Ω_D, i.e. of the solid angle under which the detector with the area $A_D = \pi R_D^2$ is seen from the scattering foil, on the other hand, turns out to be somewhat more difficult. The exact calculation Ω_{D2} (see figure 11) yields elliptic integrals which can be solved only numerically. Assuming $A_D \ll R^2 = R_A^2 + x^2$ we obtain the following approximation:

$$\Omega_{D1} = \frac{\pi R_D^2 x}{(x^2 + R_A^2)^{3/2}} \,. \tag{42}$$

The results are shown in figure 11. For $x \geq 17\,\mathrm{mm}$ the relative error is less than 1%.

7.4 Specific energy loss and stopping power

7.4.1 Theory

When charged particles pass through matter, they suffer some loss of energy and a change in direction. This is caused by the following interaction processes with the target atoms:

1. inelastic collisions with the electrons
2. elastic collisions with the atomic nuclei (Rutherford scattering)

Process (1) leads to excitation or ionization of the target atoms (electronic energy loss), while process (2) (nuclear energy loss) leads mainly to displacement of the target atoms (radiation damage) and change of direction of the incident particles. The energy loss per path length (specific energy loss) increases with decreasing energy, reaches a maximum and then drops steeply at the end of the range of the particles (see figure 13). Due to the statistical character of the processes, the incident particle beam suffers energy and angular straggling. For heavy charged particles ($m_T \gg m_e$) the nuclear energy loss is negligible above about 1 MeV per nucleon.

Figure 12 shows the share of nuclear energy loss in the total energy loss in % for the bombardment of air and gold with α particles. The nuclear share is smaller than 1% for particle energies E_T larger than 200 keV. Thus, for our experiment, the electronic energy loss is the significant process. Bethe and Bloch derived a formula for the electronic energy loss $\mathrm{d}E$ per path length unit $\mathrm{d}x$ in a correct quantum mechanical calculation (Bethe-Bloch

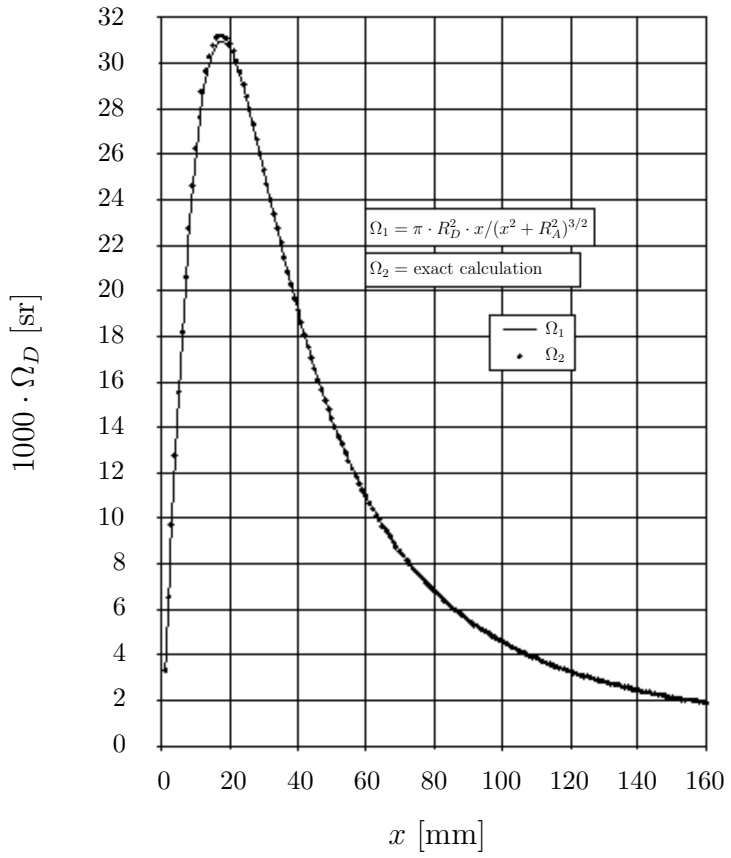

Figure 11: Detector solid angle Ω_D.

formula), which can be written in a nonrelativistic approximation in the following form:

$$-\frac{\mathrm{d}E}{\mathrm{d}x} = \frac{2\pi z^2 (e^2/(4\pi\varepsilon_0))^2}{E_T} \frac{m_T}{m_e} n_e \ln\left(\frac{4E_T}{\langle E_B\rangle \frac{m_T}{m_e}} - K\right), \tag{43}$$

or

$$-\frac{1}{N}\frac{\mathrm{d}E}{\mathrm{d}x} = \varepsilon = \frac{2\pi z^2 (e^2/(4\pi\varepsilon_0))^2}{E_T} \frac{m_T}{m_e} Z \ln\left(\frac{4E_T}{\langle E_B\rangle \frac{m_T}{m_e}} - K\right). \tag{44}$$

The quantities $-\frac{\mathrm{d}E}{\mathrm{d}x}$ or $-\frac{1}{N}\frac{\mathrm{d}E}{\mathrm{d}x}$ or $-\frac{1}{\rho}\frac{\mathrm{d}E}{\mathrm{d}x}$ are called stopping power for the corresponding particle-target combination. Depending on the definition, different units are obtained. The quantities used here are listed in table 3.

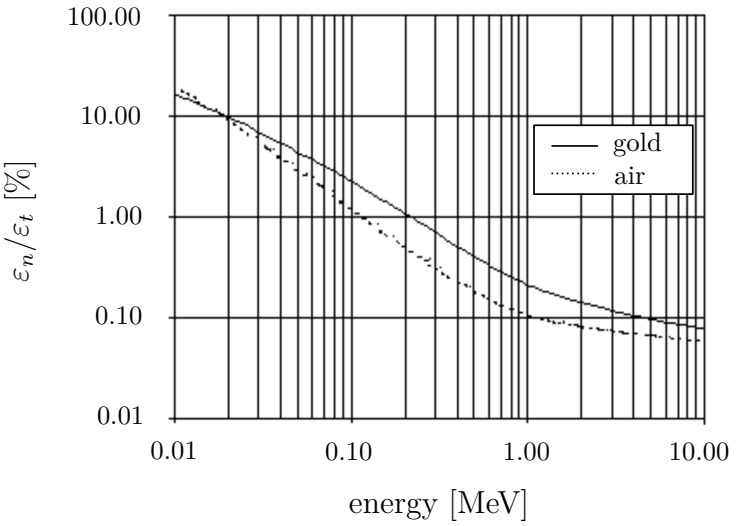

Figure 12: Share of nuclear stopping power ε_n in total stopping power ε_t for α particles in air and gold (see [7]).

Table 3: List of symbols and quantities used in the Bethe-Bloch formula.

Symbol	**Quantity**	**Value**	**Unit**
e	elementary charge	-1.602×10^{-19}	A s
$m_e c^2$	electron rest energy	0.511	MeV
N_A	Avogadro constant	6.022×10^{23}	1/mol
ε_0	dielectric constant	8.85×10^{-12}	As/Vm
$\xi^2 = \frac{e^2}{4\pi\varepsilon_0}$		1.44	eV nm
u	atomic mass unit	931.494	MeV/c^2
z	atomic number of the incident particle		
m_T	mass of the incident particle		
E_T	energy of the incident particle		
Z	atomic number of the target atoms		
$\langle E_B \rangle$	average ionization potential		
$n_e = N \cdot Z$	electron density of the target		
$N = \rho N_A / M$	number density of target atoms	gold: 5.91×10^{22}	cm^{-3}
ρ	volume density of the target		
M	molar mass of the target atoms		
K	correction constant		

For α particles we thus get:

$$-\frac{1}{N}\left(\frac{\mathrm{d}E}{\mathrm{d}x}\right)_\alpha = \varepsilon = \frac{3.80}{E_\alpha/\mathrm{MeV}} Z \ln\left(\frac{548.58(E_\alpha/\mathrm{MeV})}{\langle E_B\rangle/\mathrm{eV}} - K\right) \frac{\mathrm{eV}}{10^{15}\mathrm{atoms\ cm^{-2}}}\,. \qquad (45)$$

The average ionization potential $\langle E_B \rangle$ and the correction constant K are determined from experiments.

If no experimental material is accessible, $\langle E_B \rangle$ can be calculated by the following approx-

Table 4: The constants $\langle E_B \rangle$ and K in the Bethe-Bloch formula for the deceleration of α particles in gold and air, determined by fitting to trim calculations [7].

Material	$\langle \boldsymbol{E_B} \rangle$ [eV]	$\boldsymbol{K}$
gold	1059.81	-1.037
air	94.22	0.710

imate formula [5]:

$$\frac{\langle E_B \rangle}{Z} = \left(12 + \frac{7}{Z}\right) \text{eV}\,, \qquad Z < 13\,, \tag{46}$$

$$\frac{\langle E_B \rangle}{Z} = \left(9.76 + 58.8 Z^{-1.19}\right) \text{eV}\,, \qquad Z \geq 13\,. \tag{47}$$

The Bethe-Bloch formula only considers the electronic energy loss. Since the nuclear energy loss increases with decreasing energy, considerable deviations occur in this range. In figure 13 the stopping power of gold for α particles is shown. For α energies larger than 1.3 MeV, the deviations are smaller than 1%.

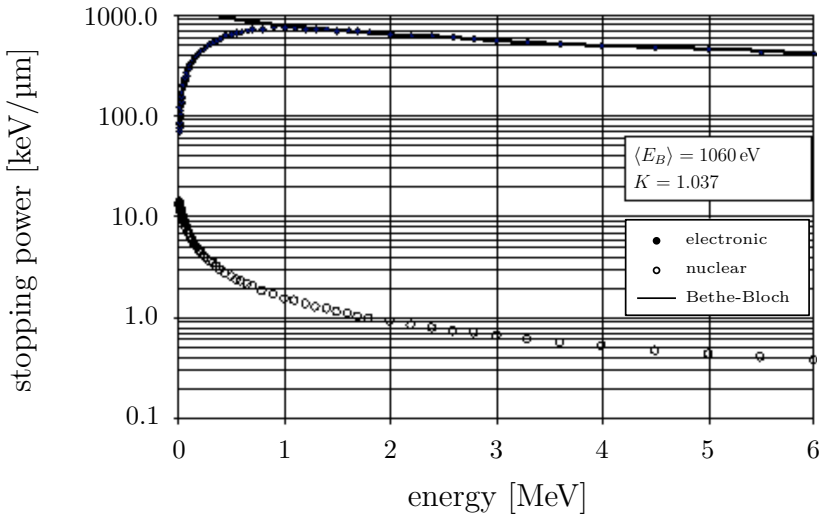

Figure 13: Stopping power of α particles in gold. For $E_\alpha > 1.3$ MeV the error of the Bethe-Bloch formula is less than 1%.

7.4.2 Energy loss in the scattering foil and in the detector entry window

The α particles hit the scattering foil with the mean energy E_0. In the scattering foil (thickness d) they are decelerated before the impact (energy loss ΔE_{in}), continue to lose energy during elastic scattering ($\Delta E_S = (1 - K_2)(E_0 - \Delta E_{\text{in}})$) and then again when leaving the foil (energy loss ΔE_{out}). Furthermore, an energy loss ΔE_D occurs in the entry window of the detector (thickness d_F). In total, this equals an energy loss of

$$\Delta E_{\text{tot}} = \Delta E_{\text{in}} + \Delta E_S + \Delta E_{\text{out}} + \Delta E_D\,. \tag{48}$$

We assume that the scattering process of α particles takes place in the center of the foil on average and that the energy loss is small, so we can put $\Delta E \cong -(\frac{\mathrm{d}E}{\mathrm{d}x}) \cdot x$ if x is the distance traveled in the particular region of the foil. This gives us the opportunity to

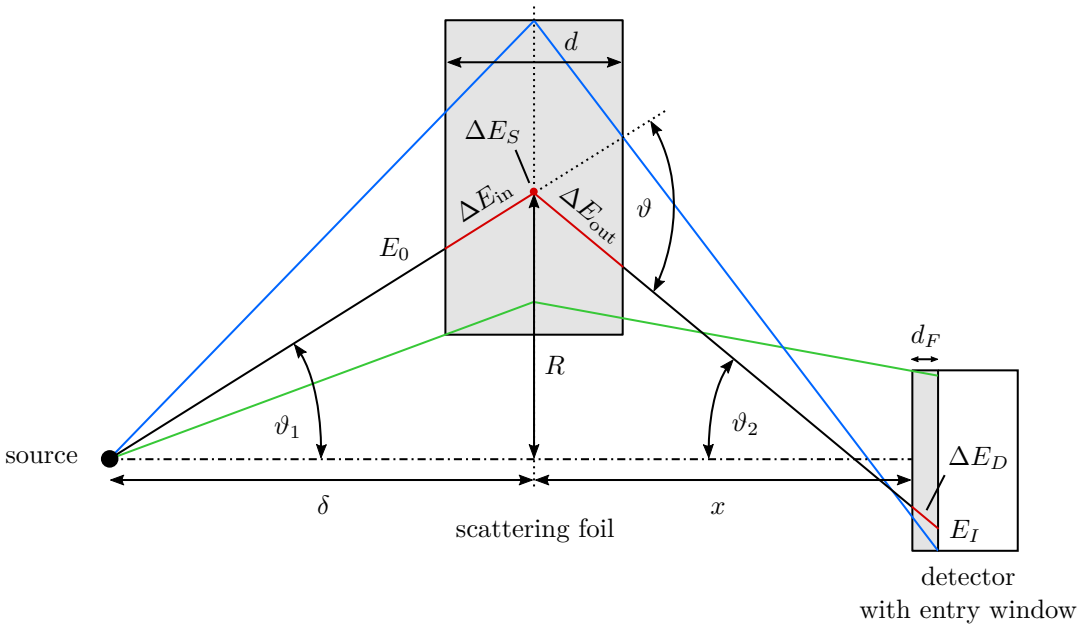

Figure 14: Scattering geometry and energy losses. The regions where energy loss occurs are indicated in red. In blue and green, respectively, the two "extreme" paths are hinted at, which are helpful for the considerations concerning the finite dimensions of the scattering geometry.

calculate the energy $E_I = E_0 - \Delta E_{\text{tot}}$ at which the α particles enter the sensitive region of the detector and to estimate the extent to which the differential cross section needs to be corrected.

7.5 Statistical analysis of the measurements

The statistical analysis of measurements is described extensively in the literature. For a quick overview we recommend [5] and [6]. We assume that we have taken measurements of a variable y at n points x_i and obtained for them the values y_i with an error of σ_i $(i = 1, 2, \ldots, n)$. We are now looking for the relationship between the quantity x and y. For this we try to fit a function $f(x; a_1, a_2, \ldots, a_m)$ with the unknown parameters a_j to our measured values, which should represent the progression of the measurements as best as possible. The number of measurements must of course be larger than the number of parameters. The parameters a_j can be determined by the method of least squares. This method states that the parameters a_j are optimally chosen if the following sum S is minimal:

$$S = \sum_{i=1}^{N} \left(\frac{y_i - f(x_j; a_j)}{\sigma_i} \right)^2 . \tag{49}$$

We see that S is just the sum of the squared deviations of the data points y_i - weighted by the squares of the corresponding errors σ_i - from the theoretical curve $f(x_i)$. Normally, it is assumed that the independent variables x_i are error-free, or that the errors in x can be neglected with respect to the errors in y. The quantities σ_i are then the errors of y_i. In cases where both errors are comparable, neglecting the errors of x leads to incorrect parameters a_j and an underdetermination of their errors. For comparable errors in x and y, the quantities σ_i must be replaced by [5]:

$$\sigma_i^2 \to \sigma_y^2 + \left(\frac{\mathrm{d}f}{\mathrm{d}x} \right)^2 \sigma_x^2 , \tag{50}$$

where σ_x and σ_y are the errors of x and y. To determine the constants a_j, the system of equations $\frac{\partial S}{\partial a_j} = 0$ must be solved. In our case we want to fit a straight line through our measurements, i.e.:

$$y = f(x) = ax + b\,. \tag{51}$$

The target quantity Y is in any case a random variable, while the influencing variable X can be random, but does not have to be. The latter means that for a fixed value X, the quantity Y can assume different (randomly distributed) values. Thereby x_i are the set values of the quantity X and y_i are the measured values of the quantity Y at the position x_i. The parameters a and b, and their errors σ_a and σ_b, can be calculated using the following equations [5]:

$$a = \frac{EB - CA}{\Delta}\,, \quad b = \frac{DC - EA}{\Delta}\,, \quad \sigma_a^2 = \frac{B}{\Delta}\,, \quad \sigma_b^2 = \frac{D}{\Delta}\,, \tag{52}$$

where $\Delta = DB - A^2$ and

$$A = \sum \frac{x_i}{\sigma_i^2}\,, \quad B = \sum \frac{1}{\sigma_i^2}\,, \quad C = \sum \frac{y_i}{\sigma_i^2}\,, \quad D = \sum \frac{x_i^2}{\sigma_i^2}\,, \quad E = \sum \frac{x_i y_i}{\sigma_i^2}\,. \tag{53}$$

In our case we can use the initial value $a = -4$ (theoretical result) to solve these equations. Furthermore, from these equations 52 and 53 it can be observed that the calculation of the means, variances, etc. is done with weights w_i which have the following form:

$$w_i = \frac{\frac{1}{\sigma_i^2}}{\sum \frac{1}{\sigma_i^2}}\,. \tag{54}$$

The denominator is used for normalization. In the case where all σ_i are equal, the expressions must be the same as in the cases without normalization. As an example, we calculate the weighted mean of the quantity X:

$$\bar{x} = \frac{\sum\limits_{i=1}^{n} \frac{x_i}{\sigma_i^2}}{\sum\limits_{i=1}^{n} \frac{1}{\sigma_i^2}} = \frac{A}{B} \quad \xrightarrow{\text{for } \sigma_i = \sigma} \quad \bar{x} = \frac{\sum\limits_{i=1}^{n} \frac{x_i}{\sigma^2}}{\sum\limits_{i=1}^{n} \frac{1}{\sigma^2}} = \frac{\frac{1}{\sigma^2} \sum\limits_{i=1}^{n} x_i}{n \frac{1}{\sigma^2}} = \frac{1}{n} \sum_{i=1}^{n} x_i\,. \tag{55}$$

We now have to investigate whether our data can actually be approximated by the function $f(x)$ (in our case a straight line) and how good this approximation is. This question can only be answered in the context of probability theory. The corresponding test is called χ^2 test. In the literature (see e.g. [5] or [6]) it is shown that under the condition that the values y_i are normally distributed with mean $f(x_i; a_j)$ and variance σ_i^2, the quantity S defined in equation 49 corresponds to the χ^2 distribution function. In our case, these conditions are satisfied. Since the quantities y_i are random, χ^2 is also a random quantity. It can be shown that χ^2 has the following probability density:

$$P_\chi(z) = \frac{\left(\frac{z}{2}\right)^{(\nu/2)-1} \exp\left(-\frac{z}{2}\right)}{2\Gamma\left(\frac{\nu}{2}\right)}\,, \tag{56}$$

where $z > 0$ and $P_\chi(z) = 0$ for $z \leq 0$. Here $\Gamma(\frac{\nu}{2})$ is the gamma function. The integer $\nu = n - m$ is the number of degrees of freedom and is the only parameter of the distribution. The quantity n is the number of our measurement points and m is the number

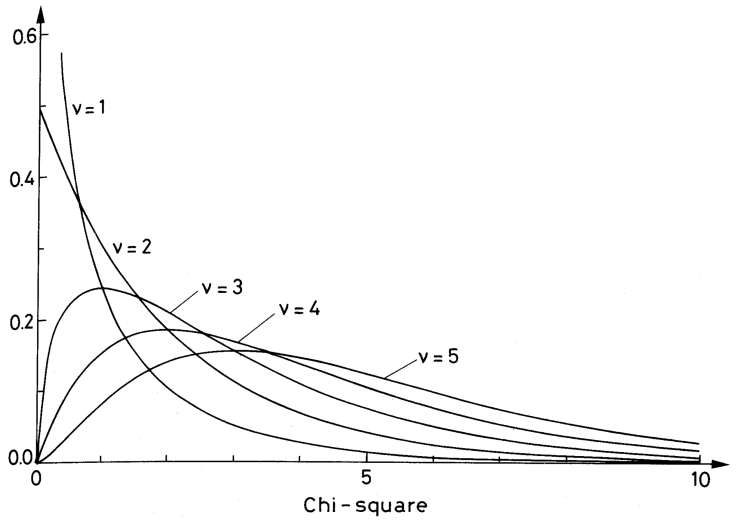

Figure 15: The χ^2 distribution ($P_\chi(z)$ as a function of $z = \chi^2$) for different values of the number of degrees of freedom ν (from [5]).

of parameters (constraints) already determined from the measurements. For example, $m = 2$ if we have determined the two parameters for the straight line equation. In figure 15, the function $P_\chi(z)$ is plotted as a function of $z = \chi^2$ for different values of ν. The mean μ and variance σ^2 of $P_\chi(z)$ equal $\mu = \nu$ and $\sigma^2 = 2\nu$.

A first and quick test for the quality of our linear fit is to calculate the quantity S itself according to equation 49. If each value y_i is just off the fit curve by σ_i, the sum should equal about n, or more precisely ν. That means for a good fit the experimentally determined reduced χ^2

$$\chi_r^2 = \frac{\chi^2}{\nu} = \frac{S}{\nu} \tag{57}$$

should approximately equal 1. Large values of S indicate that either the y_i values scatter too much or the errors were estimated to be too small. A value of S that is too small, on the other hand, means that either the errors σ_i were overestimated or the values y_i do not scatter sufficiently, e.g. that they were deliberately altered to achieve good results or that the detection electronics are defective. Since the values y_i obey a normal distribution, about 1/3 of the measured values ($y_i \pm \sigma_i$) should lie outside the fit curve! However, a more detailed analysis of our measurement and the fit of the measured values requires statistical considerations. We proceed similarly to the error function $\Phi(z)$ which has a normal distribution (Gaussian distribution) as probability density. The starting point is the question (hypothesis H_0) whether an (empirical) distribution obtained in the experiment deviates only by chance from a theoretical distribution given a certain probability of error α. As a test variable we use χ^2, which expresses the deviation between empirical and theoretical distribution, and ask for the probability to find χ^2 within certain limits. We will explain the general procedure with an example. The result of our scattering measurement is shown in figure 16.

We now specify e.g. a probability of error of $\alpha = 0.05$ (5%). On the basis of our measurement (sample) we now try to specify an interval J which covers χ^2 with a probability as large as possible. If we denote this probability (confidence level) with $q = 1 - \alpha$ and the boundaries of the interval J with G_u and G_o, i.e. if $J = (G_u, G_o)$ with $G_u < G_o$ holds,

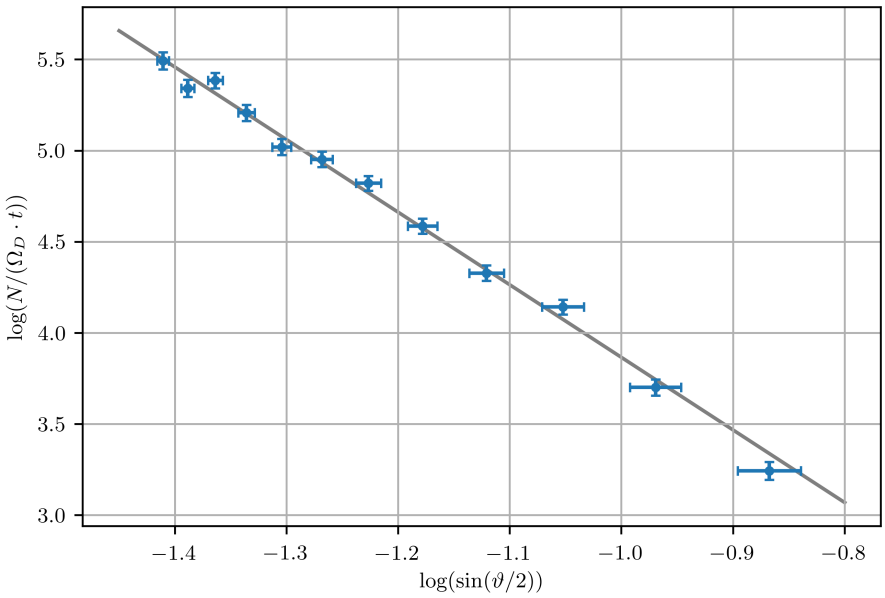

Figure 16: Scattering measurement with $n = 12$ measurement points and the fit curve $y = ax + b$, with $a = -3.98$, $\sigma_a = 0.14$, $b = -0.12$, $\sigma_b = 0.03$, $\nu = 12 - 2 = 10$, $S = 7.15$, $S/\nu = 0.715$.

this requirement means:

$$P(\chi^2 \geq G_u) = \int_{G_u}^{\infty} P_\chi(z)\mathrm{d}z = 1 - \frac{\alpha}{2} \tag{58}$$

and

$$P(\chi^2 \geq G_o) = \int_{G_o}^{\infty} P_\chi(z)\mathrm{d}z = \frac{\alpha}{2}\,. \tag{59}$$

Combining both requirements yields

$$P(G_u < \chi^2 < G_o) = \int_{G_u}^{G_o} P_\chi(z)\mathrm{d}z = q = 1 - \alpha\,. \tag{60}$$

Figure 17 illustrates this relation for the χ^2 distribution with $\nu = 6$ degrees of freedom. The limits G_u and G_o are obtained by cutting off the area $\frac{\alpha}{2}$ on both sides under the curve in the graph of the (asymmetric) density $P_\chi(z)$ of the χ^2 distribution. Thus we obtain for the confidence limits:

$$G_u = \chi^2_{\nu;1-\frac{\alpha}{2}}\,, \quad G_o = \chi^2_{\nu;\frac{\alpha}{2}}\,. \tag{61}$$

The values $\chi^2_{\nu;q}$ can be obtained from the table for the χ^2 distribution. Equation 60 can be interpreted as follows: Out of 100 calculated confidence intervals obtained from samples of the same population with parameter $S = \chi^2$, on average $(1-\alpha)\cdot 100 = q \cdot 100$ overlap the true parameter χ^2. Only $100 \cdot \alpha$ of all samples on average provide bounds that do not contain χ^2. For our example in figure 16 ($\nu = 10$ and $\alpha = 0.05$), we extract the values of $G_u/\nu = \chi^2_r = \chi^2_{\nu;1-\frac{\alpha}{2}}/\nu = 0.32$ and $G_u/\nu = \chi^2_r = \chi^2_{\nu;\frac{\alpha}{2}}/\nu = 2.07$ from table 5 by linear interpolation. We have obtained $S/\nu = 0.715$ as the experimental value. This value is within the given limits, so we can accept our hypothesis H_0 that our measurement points can be approximated by the calculated fit curve.

In general, it is assumed that for values of P between 0.1 and 0.9 the fit is acceptable, whereas for $P < 0.02$ and $P > 0.98$ the results are highly questionable and need to be verified.

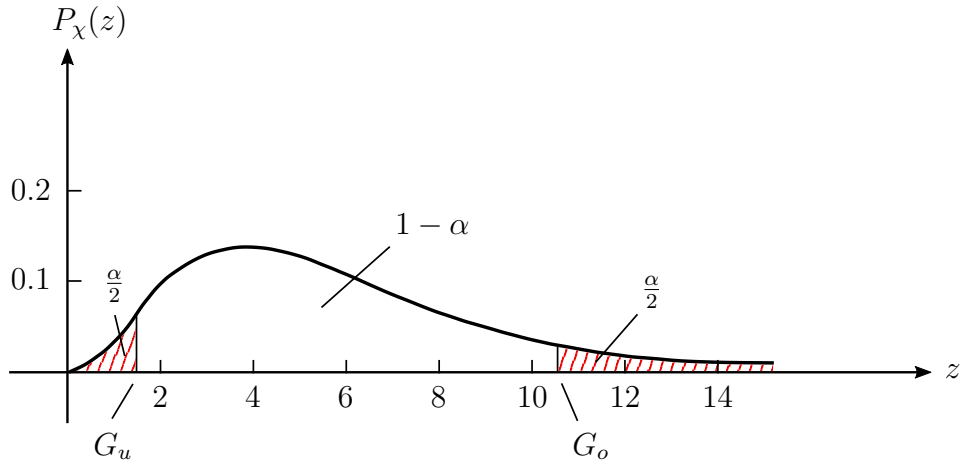

Figure 17: Confidence limits for χ^2 with probability of error α.

Table 5: χ^2 distribution (see [6]) for $0.99 \geq \alpha \geq 0.001$. Values of $\chi^2_r = \chi^2_{\nu;q}/\nu$ corresponding to the probability $P(\chi^2 > \chi^2_{\nu;q}) = \alpha$ that $\chi^2_{\nu;q}$ is exceeded.

ν	**0.99**	**0.98**	**0.95**	**0.90**	**0.80**	**0.70**	**0.60**	**0.50**
1	0.00016	0.00063	0.00393	0.0158	0.0642	0.148	0.275	0.455
2	0.0100	0.0202	0.0515	0.105	0.223	0.357	0.511	0.693
3	0.0383	0.0617	0.117	0.195	0.335	0.475	0.623	0.789
4	0.0742	0.107	0.178	0.266	0.412	0.549	0.688	0.839
5	0.111	0.150	0.229	0.322	0.469	0.600	0.731	0.870
6	0.145	0.189	0.273	0.367	0.512	0.638	0.762	0.891
7	0.177	0.223	0.310	0.405	0.546	0.667	0.785	0.907
8	0.206	0.254	0.342	0.436	0.574	0.691	0.803	0.918
9	0.232	0.281	0.369	0.463	0.598	0.710	0.817	0.927
10	0.256	0.306	0.394	0.487	0.618	0.727	0.830	0.934
11	0.278	0.328	0.416	0.507	0.635	0.741	0.840	0.940
12	0.298	0.348	0.436	0.525	0.651	0.753	0.848	0.945
13	0.316	0.367	0.453	0.542	0.664	0.764	0.856	0.949
14	0.333	0.383	0.469	0.556	0.676	0.773	0.863	0.953
15	0.349	0.399	0.484	0.570	0.687	0.781	0.869	0.956
16	0.363	0.413	0.498	0.582	0.697	0.789	0.874	0.959
17	0.377	0.427	0.510	0.593	0.706	0.796	0.879	0.961
18	0.390	0.439	0.522	0.604	0.714	0.802	0.883	0.963
19	0.402	0.451	0.532	0.613	0.722	0.808	0.887	0.965
20	0.413	0.462	0.543	0.622	0.729	0.813	0.890	0.967

ν	**0.40**	**0.30**	**0.20**	**0.10**	**0.05**	**0.02**	**0.01**	**0.001**
1	0.708	1.074	1.642	2.706	3.841	5.412	6.635	10.827
2	0.916	1.204	1.609	2.303	2.996	3.912	4.605	6.908
3	0.982	1.222	1.547	2.084	2.605	3.279	3.780	5.423
4	1.011	1.220	1.497	1.945	2.372	2.917	3.319	4.617
5	1.026	1.213	1.458	1.847	2.214	2.678	3.017	4.102
6	1.035	1.205	1.426	1.774	2.099	2.506	2.802	3.743
7	1.040	1.198	1.400	1.717	2.010	2.375	2.639	3.475
8	1.044	1.191	1.379	1.670	1.938	2.271	2.511	3.266
9	1.046	1.184	1.360	1.632	1.880	2.187	2.407	3.097
10	1.047	1.178	1.344	1.599	1.831	2.116	2.321	2.959
11	1.048	1.173	1.330	1.570	1.789	2.056	2.248	2.842
12	1.049	1.168	1.318	1.546	1.752	2.004	2.185	2.742
13	1.049	1.163	1.307	1.524	1.720	1.959	2.130	2.656
14	1.049	1.159	1.296	1.505	1.692	1.919	2.082	2.580
15	1.049	1.155	1.287	1.487	1.666	1.884	2.039	2.513
16	1.049	1.151	1.279	1.471	1.644	1.852	2.000	2.453
17	1.048	1.148	1.271	1.457	1.623	1.823	1.965	2.399
18	1.048	1.145	1.264	1.444	1.604	1.797	1.934	2.351
19	1.048	1.142	1.258	1.432	1.586	1.773	1.905	2.307
20	1.048	1.139	1.252	1.421	1.571	1.751	1.878	2.266

References

[1] H. Geiger and E. Marsden. LXI. The laws of deflexion of a particles through large angles. *The London, Edinburgh, and Dublin Philosophical Magazine and Journal of Science*, 25(148):604–623, 1913.
doi: https://doi.org/10.1080/14786440408634197.

[2] E. Rutherford. LXXIX. The scattering of α and β particles by matter and the structure of the atom. *The London, Edinburgh, and Dublin Philosophical Magazine and Journal of Science*, 21(125):669–688, 1911.
doi: https://doi.org/10.1080/14786440508637080.

[3] L.C. Feldman and J.W. Mayer. *Fundamentals of Surface and Thin Film Analysis*. North-Holland, New York, 1986.

[4] T. Mayer-Kuckuk. *Kernphysik*. Vieweg+Teubner Verlag, Wiesbaden, 1992.
doi: https://doi.org/10.1007/978-3-322-91795-9.

[5] W.R. Leo. *Techniques for Nuclear and Particle Physics Experiments*. Springer, Berlin, Heidelberg, 1994.
doi: https://doi.org/10.1007/978-3-642-57920-2.

[6] P.R. Bevington and D.K. Robinson. *Data reduction and error analysis for the physical sciences*. McGraw-Hill, New York, 1992.

[7] J.F. Ziegler, J.P. Biersack, and U. Littmark. *The Stopping and Range of Ions in Solids*. Pergamon Press, New York, 1985.

[8] Y.A. Akovali. Nuclear Data Sheets for A = 237. *Nuclear Data Sheets*, 74(3):461–527 (505), 1995.
doi: https://doi.org/10.1006/ndsh.1995.1014.

List of Figures

List of Tables